

Quantum transport in ballistic conductors: evolution from conductance quantization to resonant tunnelling

This article has been downloaded from IOPscience. Please scroll down to see the full text article.

2000 J. Phys.: Condens. Matter 12 9629

(<http://iopscience.iop.org/0953-8984/12/46/310>)

View [the table of contents for this issue](#), or go to the [journal homepage](#) for more

Download details:

IP Address: 171.66.16.221

The article was downloaded on 16/05/2010 at 06:59

Please note that [terms and conditions apply](#).

Quantum transport in ballistic conductors: evolution from conductance quantization to resonant tunnelling

Branislav K Nikolić and Philip B Allen

Department of Physics and Astronomy, SUNY at Stony Brook, Stony Brook, NY 11794-3800, USA

Received 31 August 2000, in final form 10 October 2000

Abstract. We study the transport properties of an atomic-scale contact in the ballistic regime. The results for the conductance and related transmission eigenvalues show how the properties of the ideal semi-infinite leads (i.e. measuring device) as well as the coupling between the leads and the conductor influence the transport in a two-probe geometry. We observe the evolution from conductance quantization to resonant tunnelling conductance peaks upon changing the hopping parameters in the disorder-free tight-binding Hamiltonian which characterize the leads and the coupling to the sample.

Mesoscopic physics [1] has changed our understanding of transport in condensed matter systems. The unearthing of new effects, such as weak localization [2] or universal conductance fluctuations [3], has been accompanied by rethinking of the established transport ideas in a new light. One of the most spectacular discoveries of mesoscopics is conductance quantization (CQ) [4, 5] in a short and narrow constriction connecting two high-mobility (ballistic) two-dimensional electron gases. The conductance of these quantum point contacts as a function of the constriction width $W \sim \lambda_F$ has steps of magnitude $2e^2/h$. New experimental techniques have made possible the observation of similar phenomena [6] in metallic point contacts of atomic size. The Landauer formula [7] for the two-probe conductance

$$G = \frac{2e^2}{h} \text{Tr}(\mathbf{t}\mathbf{t}^\dagger) = G_Q \sum_{n=1}^N T_n \quad (1)$$

has provided an explanation of the stepwise conductance in terms of the number N of transverse propagating states ('channels') at the Fermi energy E_F which are populated in the constriction. Here \mathbf{t} is the transmission matrix, T_n transmission eigenvalues and $G_Q = 2e^2/h$ is the conductance quantum. In the ballistic case $(\mathbf{t}\mathbf{t}^\dagger)_{ij}$ is δ_{ij} , or equivalently T_n is 1. Further studies have explored CQ under a range of conditions [8]. They include various geometries [9, 10], scattering on impurities [11], temperature effects, and magnetic field.

In this paper we study the influence of the attached leads on ballistic transport ($\ell > L$, ℓ being elastic mean free path, L being the system size) in a nanocrystal. We assume that in the two-probe measuring geometry an electron leaving the sample does not re-enter the sample in a phase-coherent way. This means that at zero temperature the phase coherence length L_ϕ is equal to the length of the sample L . In the jargon of quantum measurement theory, the leads act as a 'macroscopic measurement apparatus'. Our concern with the influence of the leads on conductance is therefore also a concern of quantum measurement theory. Recently, the effects

of a lead–sample contact on quantum transport in molecular devices have received increased attention in the developing field of ‘nanoelectronics’ [12]. Also, the simplest lattice model and related real-space Green function technique are chosen here in order to address some practical issues which appear in the frequent use of these methods [1] to study transport in disordered samples. We emphasize that the relevant formulae for transport coefficients contain three different energy scales (introduced by the leads, the sample, and the lead–sample contact), as discussed below.

In order to isolate just these effects we pick the strip geometry in the two-probe measuring set-up shown in figure 1.

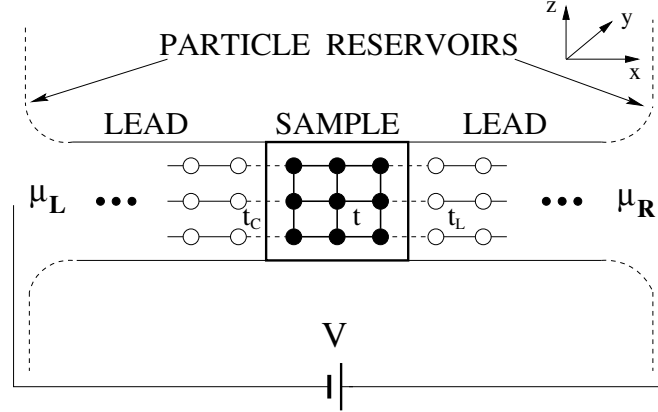


Figure 1. A two-dimensional version of our actual 3D model of a two-probe measuring geometry. Each site hosts a single s orbital which hops to six (or fewer for surface atoms) nearest neighbours. The hopping matrix element is t (within the sample), t_L (within the leads), and t_C (coupling of the sample to the leads). The leads are semi-infinite and connected at $\pm\infty$ to reservoirs biased by the potential difference $\mu_L - \mu_R = eV$.

The three-dimensional (3D) nanocrystal (‘sample’) is placed between two ideal (disorder-free) semi-infinite ‘leads’ which are connected to macroscopic reservoirs. The electrochemical potential difference $eV = \mu_L - \mu_R$ is measured between the reservoirs. The leads have the same cross section as the sample. This eliminates scattering induced by the wide-to-narrow geometry [10] of the sample–lead interface. The whole system is described by a clean tight-binding Hamiltonian (TBH) with nearest-neighbour hopping parameters t_{mn} :

$$\hat{H} = \sum_{(m,n)} t_{mn} |m\rangle \langle n| \quad (2)$$

where $|m\rangle$ is the orbital $\psi(\mathbf{r} - \mathbf{m})$ on the site \mathbf{m} . The ‘sample’ is the central section with $N_x \times N_y \times N_z$ sites, and for simplicity and clarity of the subsequent results a small lattice for this section is chosen. The ‘sample’ is perfectly ordered with $t_{mn} = t$. The leads are the same except that $t_{mn} = t_L$. Finally, the parameter describing the hopping (coupling) between the sample and the lead is $t_{mn} = t_C$. We use hard-wall boundary conditions in the \hat{y} - and \hat{z} -directions. The different hopping parameters introduced here are necessary when studying disordered samples in the same geometry—to get the conductance at the Fermi energies throughout the whole band extended (compared to the clean case) by disorder one has to use [13] $t_L > t$. Thus, one should be aware of the conductances we calculate in the rest of the paper when engaging in such studies.

Our toy model shows exact conductance steps in multiples of G_Q when $t_C = t_L = t$. This is a consequence of infinitely smooth (‘ideally adiabatic’ [9]) sample–lead geometry.

Then we study the evolution of quantized conductance into resonant tunnelling conductance while changing the parameter t_L of the leads as well as the coupling between the leads and the conductor t_C . An example of this evolution is given in figure 2. The equivalent evolution of the transmission eigenvalues T_n of channels is shown in figure 3. A similar evolution has been studied recently in one-atom point contacts [14].

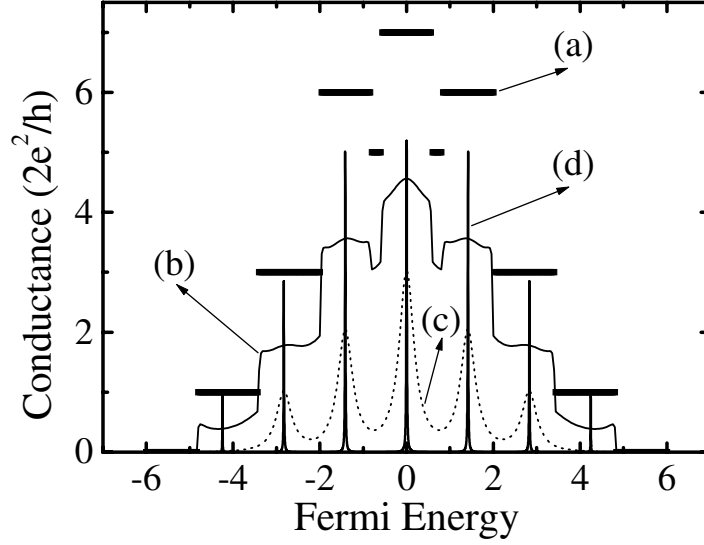


Figure 2. The conductance G of a ballistic conductor modelled on a simple cubic lattice, $3 \times 3 \times 3$, for the following values of the lead and coupling parameters: (a) $t_C = 1$, $t_L = 1$; (b) $t_C = 1.5$, $t_L = 1$; (c) $t_C = 3$, $t_L = 1$; and (d) $t_C = 0.1$, $t_C = 1$. In the case (d), the conductance peaks are connected by smooth curves of $G < 0.004e^2/h$.

The non-zero resistance is a purely geometrical effect [15] caused by reflection when the large number of channels in the macroscopic reservoirs matches the small number of channels in the lead, and is known (in a non-quantized form) from the studies of classical point contacts [16, 17]. The sequence of steps (1, 3, 6, 5, 7, 5, 6, 3, 1 multiples of G_Q as the Fermi energy E_F is varied) is explained as follows. The eigenstates in the leads, which comprise the scattering basis, have the form $\psi_k \propto \sin(k_y m_y) \sin(k_z m_z) e^{ik_x m_x}$ at atom m , with energy $E = 2t_L[\cos(k_x a) + \cos(k_y a) + \cos(k_z a)]$, where a is the lattice constant. The discrete values $k_y(i) = i\pi/(N_y + 1)a$ and $k_z(j) = j\pi/(N_z + 1)a$ define subbands or ‘channels’ labelled by $(k_y, k_z) \equiv (i, j)$, where i runs from 1 to N_y and j runs from 1 to N_z . The channel (k_y, k_z) is open if E_F lies between the bottom of the subband, $2t_L[-1 + \cos(k_y a) + \cos(k_z a)]$, and the top of the subband, $2t_L[1 + \cos(k_y a) + \cos(k_z a)]$. Because of the degeneracy of different transverse modes in 3D, several channels (k_y, k_z) open or close at the same energy. Each channel contributes one conductance quantum G_Q . This is shown in figure 2 for a sample with 3×3 cross section where the number of transverse propagating modes at E_F (‘open channels’) is $N < 9$. In the adiabatic geometry channels do not mix, i.e. the transmission matrix is diagonal in the basis of channels defined by the leads. Nevertheless, adiabaticity does not ensure CQ with backscattering present [18], as demonstrated when the hopping parameters (t , t_L , and t_C) differ from each other.

We compute the conductance using the expression obtained in the framework of the Keldysh technique [19]. This provides the following Landauer-type formula for the

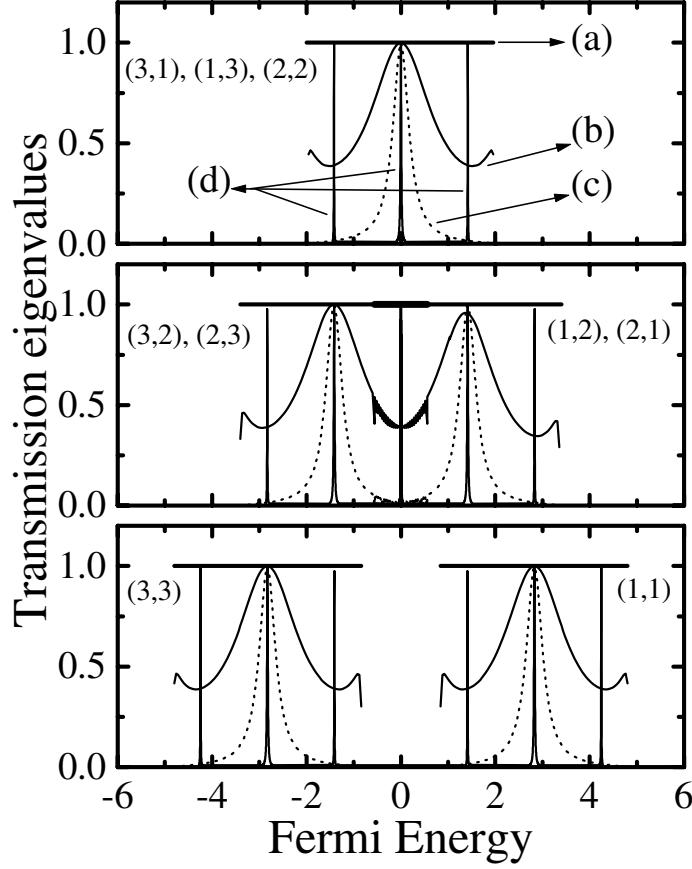


Figure 3. Transmission eigenvalues of a ballistic conductor modelled on a simple cubic lattice, $3 \times 3 \times 3$. The parameters t_L and t_C are the same as in figure 2. All channels $(i, j) \equiv (k_y(i), k_z(j))$ whose subbands are identical have the same T_n . This gives the degeneracy of T_n : three (upper panel), two (middle panel), and one (bottom panel). In the middle panel the lower two subbands have an energy interval of overlap with the upper two subbands.

conductance of a non-interacting system:

$$G = \frac{2e^2}{h} \text{Tr}(\hat{\Gamma}_L \hat{G}_{1N_x}^r \hat{\Gamma}_R \hat{G}_{N_x 1}^a) = \frac{2e^2}{h} \text{Tr}(\mathbf{t}\mathbf{t}^\dagger) \quad (3)$$

$$\mathbf{t} = \sqrt{\hat{\Gamma}_L} \hat{G}_{1N_x}^r \sqrt{\hat{\Gamma}_R}. \quad (4)$$

Here $\hat{G}_{1N_x}^r, \hat{G}_{N_x 1}^a$ are matrices whose elements are the Green functions connecting the layers 1 and N_x of the sample. Therefore, only the $N_y \times N_z$ block of the complete matrix $\hat{G}(\mathbf{n}, \mathbf{m})$ is needed to compute the conductance. The expression (3) is formally equivalent to that (1) of the Landauer–Büttiker scattering formalism [1]. It provides the exact zero-temperature conductance and allows us to treat any lead–sample coupling [19]. Such Landauer-type expressions, based on single-particle Green functions, are commonly used in the literature [1, 20, 21] because of the computational efficiency of (often real-space) Green function techniques (in particular, these techniques have the advantage of being useful even in the situations where it becomes hard to define the asymptotic conducting channels [22]).

We employ this (somewhat too sophisticated for our simple problem) computational scheme in order to take into account different energy scales present in the lattice Hamiltonians, like (2), which are usually not treated explicitly in application of such methods to more complicated systems.

The positive operator $\hat{\Gamma}_L = i(\hat{\Sigma}_L^r - \hat{\Sigma}_L^a) = -2 \text{Im} \hat{\Sigma}_L > 0$ in (3) is the counterpart of the spectral function $\hat{A} = i(\hat{G}^r - \hat{G}^a)$ for the ‘self-energy’ $\hat{\Sigma}_L$ introduced by the left lead. It ‘measures’ the coupling of the open sample to the left lead ($\hat{\Gamma}_R$ is equivalent for the right lead). The Green operator is defined as the inverse of $(E - \hat{H})$ including the relevant boundary conditions. Instead of inverting the infinite matrix we invert only $(E - \hat{H}_S)$ defined on the Hilbert space spanned by orbitals $|\mathbf{m}\rangle$ inside the sample [19]:

$$\hat{G}^r = (E - \hat{H}_S - \hat{\Sigma}^r)^{-1} \quad (5)$$

where \hat{H}_S is the TBH for the sample only. This is achieved by using the retarded self-energy $\hat{\Sigma}^r = \hat{\Sigma}_L^r + \hat{\Sigma}_R^r$ introduced by the left (L) and the right (R) lead. In site representation, the Green operator $\hat{G}^{r,a}$ is a Green function matrix $\hat{G}^{r,a}(n, \mathbf{m}) = \langle n | \hat{G}^{r,a} | \mathbf{m} \rangle$. Equation (5) does not need the small imaginary part $i0^+$ necessary to specify the retarded or advanced Green operator $\hat{G}^{r,a}$ because the lead self-energy ($\hat{\Sigma}^a = [\hat{\Sigma}^r]^\dagger$) adds a well defined imaginary part to $E - \hat{H}_S$. This imaginary part is related to the average time that an electron spends inside the sample before escaping into the leads. The self-energy terms have non-zero matrix elements only on the edge layers of the sample adjacent to the leads. They are given [20] in terms of the Green function on the lead edge layer and the coupling parameter t_C :

$$\hat{\Sigma}_{L,R}^r(n, \mathbf{m}) = \frac{2}{N_y + 1} \frac{2}{N_z + 1} \sum_{k_y, k_z} \sin(k_y n_y a) \sin(k_z n_z a) \hat{\Sigma}^r(k_y, k_z) \sin(k_y m_y a) \sin(k_z m_z a) \quad (6)$$

where (n, \mathbf{m}) is the pair of sites on the surfaces inside the sample which is adjacent to the leads L or R . The self-energy $\hat{\Sigma}^r(k_y, k_z)$ of the channel (k_z, k_y) is given by

$$\hat{\Sigma}^r(k_y, k_z) = \frac{t_C^2}{2t_L^2} \left(E_\Sigma - i\sqrt{4t_L^2 - E_\Sigma^2} \right) \quad (7)$$

for $|E_\Sigma| < 2t_L$. We use the shorthand notation $E_\Sigma = E - \varepsilon(k_y, k_z)$, where $\varepsilon(k_y, k_z) = 2t_L[\cos(k_y a) + \cos(k_z a)]$ is the energy of quantized transverse levels in the lead. In the opposite case, $|E_\Sigma| > 2t_L$, we have

$$\hat{\Sigma}^r(k_y, k_z) = \frac{t_C^2}{2t_L^2} \left(E_\Sigma - \text{sgn} E_\Sigma \sqrt{E_\Sigma^2 - 4t_L^2} \right). \quad (8)$$

In order to study the conductance as a function of two parameters t_L and t_C , we change either one of them while holding the other fixed (at the unit of energy specified by t), or both at the same time. The first case is shown in figure 2 and figure 4 (upper panel), while the second one is shown in figure 4 (lower panel). The conductance is depressed in all cases since these configurations of hopping parameters t_{mn} effectively act as a barriers. There is a reflection at the sample–lead interface due to the mismatch of the subbands in the lead and in the sample when t_L differs from t . In general, each set of channels which have the same energy subband is characterized by its own transmission function $T_n(E_F)$. When the coupling $t_C = 0.1$ is small a double-barrier structure is obtained which has a resonant tunnelling conductance. The electron tunnels from one lead to the other via discrete eigenstates. The transmission function is composed of peaks centred at $E_r = 2t[\cos(k_x a) + \cos(k_y a) + \cos(k_z a)]$, where $k_x = k\pi/(N_x + 1)a$ is now quantized inside the sample, i.e. k runs from 1 to N_x . The magnitude and width of the peaks are defined by the rate at which an electron placed between

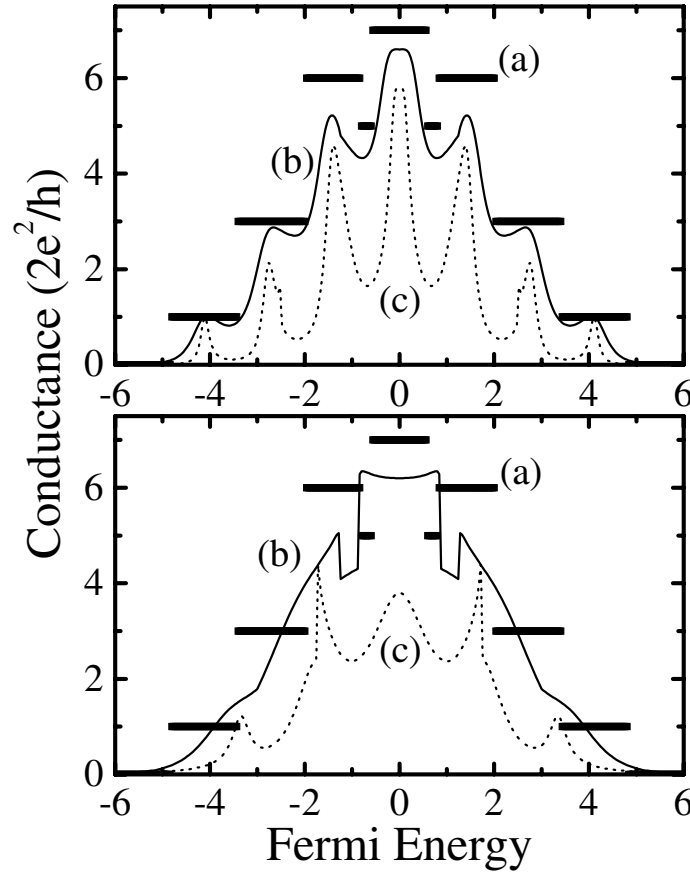


Figure 4. Conductance G of a ballistic conductor modelled on a simple cubic lattice, $3 \times 3 \times 3$, for the following values of the lead and coupling parameters: upper panel—(a) $t_C = 1$, $t_L = 1$; (b) $t_C = 1$, $t_L = 1.5$; and (c) $t_C = 1$, $t_L = 3$; lower panel—(a) $t_C = 1$, $t_L = 1$; (b) $t_C = 1.5$, $t_L = 1.5$; and (c) $t_C = 3$, $t_L = 3$.

barriers leaks out into the lead. These rates are related to the level widths generated through the coupling to the leads. In our model they are energy (i.e. mode) dependent. For example around $E_F = 0$ seven transmission eigenvalues are non-zero (in accordance with the number of open channels in figure 3) and exactly at $E_F = 0$ three of them have $T_n = 1$ and four $T_n = 0.5$. Upon decreasing t_C further, all conductance peaks, except the one at $E_F = 0$, become negligible. Singular behaviour of $G(E_F)$ at subband edges of the leads was observed before [11].

It is worth mentioning that the same results are obtained using a non-standard version of the Kubo–Greenwood formula [23] for the volume-averaged conductance:

$$G = \frac{4e^2}{h} \frac{1}{L_x^2} \text{Tr}(\hbar \hat{v}_x \text{Im} \hat{G} \hbar \hat{v}_x \text{Im} \hat{G}) \quad (9a)$$

$$\text{Im} \hat{G} = \frac{1}{2i} (\hat{G}^r - \hat{G}^a) \quad (9b)$$

where v_x is the x -component of the velocity operator. The formula was originally derived for an infinite system without any notion of leads and reservoirs. The crucial non-standard

aspect is the use of the Green function (5) in the formula (9). This takes into account, through lead self-energy (6), the boundary conditions at the reservoirs. The reservoirs are necessary in both Landauer and Kubo formulations of linear transport for open finite systems. They provide thermalization and therefore a steady state of the transport in the central region. Using semi-infinite leads [24] is a convenient method for taking into account electrons entering or leaving the phase-coherent sample, thereby allowing us to bypass explicit modelling of the thermodynamics of macroscopic reservoirs. The equivalence between this ‘non-standard’ Kubo formula for the finite-size system and the Landauer formula (which takes into account the finite size of the sample from the outset) is a well established fact [25]. Here we just want to emphasize that when employing the Kubo formula (9) one can (and should) use current conservation and compute the trace only on two adjacent layers inside the sample. Inasmuch as the velocity operator $i\hbar\hat{v}_x = [\hat{x}, \hat{H}]$ for the nearest-neighbour TBH (2) connecting the states residing on two adjacent layers is non-zero, the computation of the Green function elements $\hat{G}^{r,a}(\mathbf{n}, \mathbf{m})$, connecting states on those two layers, represents the minimum of the computational complexity in this method [20] (together with subsequent trace over those two layers). This is obviously a bit more ‘complex’ (and time consuming) than the use of the equivalent Landauer-type formula (3). To get the correct results in this scheme, L_x in equation (9) should be replaced by a lattice constant a . It is interesting that if one traces in the ‘pedestrian way’ over the whole conductor (as ‘suggested’ by (9) at first sight), the denominator should contain the number of pairs of adjacent layers $(N - 1)a$ instead of $L_x = Na$.

In the quantum transport theory of disordered systems the influence of the leads on the conductance of a sample is understood as follows [26]. An isolated sample has a discrete energy spectrum. Attaching leads necessary for transport measurements will broaden energy levels. If the level width Γ due to the coupling to leads is larger than the Thouless energy $E_{\text{Th}} = \hbar/\tau_{\mathcal{D}} \simeq \hbar\mathcal{D}/L^2$ ($\mathcal{D} = v_F\ell/3$ being the diffusion constant), the level discreteness is unimportant for transport. For our case of ballistic conduction, E_{Th} is replaced by the inverse time of flight $\hbar v_F/L$. In the disordered sample where $\Gamma \gg E_{\text{Th}}$, varying the strength of the coupling to the leads will not change the transport coefficients. In other words, the intrinsic resistance of the sample is much larger than the resistance of the lead–sample contact [27]. In the opposite case, discreteness of levels becomes important and the strength of the coupling defines the conductance. This is the realm of quantum dots [28] where weak enough coupling can make the charging energy $e^2/2C$ of a single electron important as well. Changing the properties of the dot–lead contact affects the conductance, i.e. the result of measurement depends on the measuring process. The decay width $\Gamma = \hbar/\tau_{\text{dwell}}$ of the electron emission into one of the leads is determined by transmission probabilities of channels through the contact and mean level spacing [26]. This means that mean dwell time τ_{dwell} inside our sample depends on both t_C and t_L . Changing the hopping parameters will make τ_{dwell} greater than the time of flight $\tau_f = L/v_F$. Thus, ballistic conductance sensitively depends on the parameters of the dephasing environment (i.e., the leads).

In conclusion, we have studied the transport properties of a ballistic nanocrystal placed between two semi-infinite leads in the simplest strip geometry. We observe extreme sensitivity of the conductance to changes in the hopping parameter in the leads as well as the coupling between the leads and the sample. As can be easily anticipated, the conductance evolves from perfect quantization to resonant tunnelling. Nevertheless, it is quite amusing that vastly different $G(E_F)$ are obtained between these two limits (see e.g. figure 4). The results are of relevance for the analogous theoretical studies of disordered conductors as well as for the experiments using clean metal junctions with different effective electron mass throughout the circuit.

Acknowledgments

This work was supported in part by NSF grant No DMR 9725037. We thank I L Aleiner for interesting discussions and criticism.

References

- [1] Datta S 1995 *Electronic Transport in Mesoscopic Systems* (Cambridge: Cambridge University Press)
- [2] Gor'kov L P, Larkin A I and Khmel'nitskii D E 1979 *Pis. Zh. Eksp. Teor. Fiz.* **30** 248 (Engl. Transl. 1979 *JETP Lett.* **30** 228)
- [3] Altshuler B L 1985 *Pis. Zh. Eksp. Teor. Fiz.* **41** 530 (Engl. Transl. 1985 *JETP Lett.* **41** 648)
Lee P A and Stone A D 1985 *Phys. Rev. Lett.* **55** 1622
- [4] van Wees B J, van Houten H, Beenakker C W J, Williamson J G, Kouwenhoven L P, van der Marel D and Foxon C T 1988 *Phys. Rev. Lett.* **60** 848
- [5] Wharam D A, Thornton T J, Newbury R, Pepper M, Ahmed H, Frost J E F, Hasko D G, Peacock D C, Ritchie D A and Jones G A C 1988 *J. Phys. C: Solid State Phys.* **21** L209
- [6] Ruitenbeek J M 1999 *Preprint cond-mat/9910394*
- [7] Landauer R 1957 *IBM J. Res. Dev.* **1** 223
Landauer R 1970 *Phil. Mag.* **21** 863
- [8] He S and Das Sarma S 1993 *Phys. Rev. B* **48** 4629
- [9] Glazman L I, Lesovick G B, Khmel'nitskii D E and Shekter R I 1988 *Pis. Zh. Eksp. Teor. Fiz.* **48** 218 (Engl. Transl. 1988 *JETP Lett.* **48** 238)
- [10] Szafer A and Stone A D 1989 *Phys. Rev. Lett.* **62** 300
- [11] Maslov D L, Barnes C and Kirczenow G 1993 *Phys. Rev. Lett.* **70** 1984
Beenakker C W J and Melsen J A 1994 *Phys. Rev. B* **50** 2450
- [12] Di Ventura M, Pantelidis S T and Lang N D 2000 *Phys. Rev. Lett.* **84** 979
- [13] Nikolić B K 2000 *Preprint cond-mat/0003057*
- [14] Yamaguchi F and Yamamoto Y 1998 *Superlatt. Microstruct.* **23** 737
- [15] Imry Y 1986 *Directions in Condensed Matter Physics* ed G Grinstein and G Mazenko (Singapore: World Scientific) p 101
- [16] Sharvin Yu V 1965 *Zh. Eksp. Teor. Fiz.* **48** 984 (Engl. Transl. 1965 *Sov. Phys.-JETP* **21** 655)
- [17] Nikolić B and Allen P B 1999 *Phys. Rev. B* **60** 3963
- [18] Büttiker M 1990 *Phys. Rev. B* **41** 7906
- [19] Caroli C, Combescot R, Nozières P and Saint-James D 1971 *J. Phys C: Solid State Phys.* **4** 916
- [20] Vergés J A 1999 *Comput. Phys. Commun.* **118** 71
- [21] Todorov T N, Briggs G A D and Sutton A P 1993 *J. Phys.: Condens. Matter* **5** 2389
- [22] Cuevas J C, Levy Yeyati A and Martín-Rodero A 1998 *Phys. Rev. Lett.* **80** 1066
- [23] Kubo R, Miyake S I and Hashitsume N 1965 *Solid State Physics* vol 17, ed F Seitz and D Turnbull (New York: Academic) p 288
- [24] Fisher D S and Lee P A 1981 *Phys. Rev. B* **23** 6851
- [25] Baranger H and Stone A D 1989 *Phys. Rev. B* **40** 8169
Sols F 1991 *Phys. Rev. Lett.* **67** 2874
Nöckel J U, Stone A D and Baranger H U 1993 *Phys. Rev. B* **48** 17 569
- [26] Weidenmüller H A 1990 *Physica A* **167** 28
- [27] Efetov K B 1997 *Supersymmetry in Disorder and Chaos* (Cambridge: Cambridge University Press)
- [28] Beenakker C W J 1997 *Rev. Mod. Phys.* **69** 731